A Wearable Respiratory Biofeedback System Based on Generalized Body Sensor Network

Guan-Zheng Liu, Ph.D., Bang-Yu Huang, M.S., and Lei Wang, Ph.D.

Institute of Biomedical and Health Engineering, Shenzhen Institutes of Advanced Technology, Chinese Academy of Sciences, Shenzhen, China.

Abstract

Wearable medical devices have enabled unobtrusive monitoring of vital signs and emerging biofeedback services in a pervasive manner. This article describes a wearable respiratory biofeedback system based on a generalized body sensor network (BSN) platform. The compact BSN platform was tailored for the strong requirements of overall system optimizations. A waist-worn biofeedback device was designed using the BSN. Extensive bench tests have shown that the generalized BSN worked as intended. In-situ *experiments with 22 subjects indicated that the biofeedback device was discreet, easy to wear, and capable of offering wearable respiratory trainings. Pilot studies on wearable training patterns and resultant heart rate variability suggested that paced respirations at abdominal level and with identical inhaling/exhaling ratio were more appropriate for decreasing sympathetic arousal and increasing parasympathetic activities.*

Key words: *generalized body sensor network (BSN), biofeedback training, wearable devices, heart rate variability*

Introduction

Biofeedback is an effective technique through which patients train themselves to acquire a set of skills, the learning of which is elaborated through the information given by a biofeedback apparatus. As a health intervention technique, biofeedback is well known to facilitate treatment for a wide variety of disorders with a psychosomatic component, including asthma, cardiovascular disorders, hypertension, cephalopathies, anxiety, and duodenal ulcers, and in many cases, the results obtained have been notably positive.[1] Current biofeedback research primarily focuses on biofeedback theory and instructions/guidelines; however, relatively little attention is being paid to the hardware platform of biofeedback apparatus. For example, most researches such as respiration biofeedback[2–6] employed bulky desktop devices and were conducted in advanced laboratory spaces, which inhibited the possibilities of low-cost and ubiquitous health intervention services.[7]

In another side of the spectrum, technology advantages on microelectronics and computing have led to the exploitations of body sensor networks (BSNs) that monitor patient's health status ubiquitously.[8] BSN is typically equipped with different sensors, such as photoplethysmography (PPG) sensor, electrocardiogram (ECG) sensor, and noninvasive blood pressure sensor, for on-body/in-body physiological measurements. Consequently, the data acquired from the multiple sensor nodes are relayed wirelessly and in real time to the master node, where the data are processed autonomously.[9] It is evident that the continuous development of BSN platforms could lead to emerging biofeedback apparatus as well as novel biofeedback applications. In this article, we introduced such a BSN platform and the integrated wearable device, which are able to offer patients advanced biofeedback services needed for affordable healthcare.

Related Work

Table 1 lists several existing BSN platforms. MIT Media Lab developed MIThril, a wearable computing platform compatible with different off-the-shelf sensors.[10] Chulsung and Chou developed an Eco platform, which is a self-contained, ultra-wearable, and expandable wireless sensor platform.[11] University of California Berkeley designed an open-source platform.[12,13] Yang and others from Imperial College London presented a bioinspired processing-on-node platform.[14] Previous arts also included a body area sensor network (BSAN) platform[15] and a phone-based platform.[16] These platforms are relatively premature, which means the reliability needs to be further improved before becoming commercially available; the compatibility is another issue that quite often limits their applications for other research groups. In the paper, we designed a generalized BSN platform (*Fig. 1*).

For biofeedback, Yokoyama with Nagoya City University developed an outline system that produces real-time sound with pitch and tempo, according to instantaneous heart rate.[17] Dozza with University of Bologna suggested audio and visual biofeedback for postural control benefits from different sensory coding, and each type of biofeedback may encourage a different type of postural sway strategy.[18] Komada with Mie University developed a novel biofeedback

This work was supported in part by the Chinese Academy of Sciences' "the 100-Talent People" program, the projects of National Natural Science Foundation of China (Grant Nos. 60932001 and 61072031), the National Basic Research (973) Program of China (Subgrant 6 of Grant No. 2010CB732606), and the Knowledge Innovation Program of the Chinese Academy of Sciences.

 DOI: 10.1089/tmj.2010.0182

Table 1. Prototype Body Sensor Network Platforms

PLATFORM	KEY FEATURES OF THE NODE BOARD	SENSOR INTERFACES	COMMUNICATION PROTOCOL	MEMORY BANK	STACKABLE	PLATFORM HIGHLIGHTS
Eco	TI-MSP430; TX Power consumption 102 mW; form factor 1.3 × 1.0 cm	Motion	2.4 GHz	N/A	N	Smallest, primary motion detections
DexterNet	TI-MSP430; TX power consumption 38 mW; form factor 3.2 × 6.6 cm	ECG, electrical impedance plethysmography	IEEE 802.15.4 MLA of UPMA	1 MB	N	One of the earliest work, Tiny-OS based, chronic disease management
Imperial BSN	TI-MSP430; TX Power consumption 18 mW; form factor 1.9 × 3.0 cm	Motion, ECG	IEEE 802.15.4 ZigBee 2.4 GHz	4 MB	Y	Tiny-OS based, surgical skill assessments
BSAN	TI-MSP430; TX Power consumption 107 mW; form factor 4.0 cm in diameter	Motion	RN41 Bluetooth	N	N	Accelerometer and gyro for motion detections
Phone-based BSN	TI-MSP430; TX Power consumption 160 mW; form factor 3.3 × 3.3 cm	ECG	KC21 Bluetooth	N	N	Efficient Bluetooth energy managements
This work	TI-MSP430; TX Power consumption 7.8 mW; form factor 2.3 cm in diameter	Motion, noncontact ECG, RIP, PPG	IEEE 802.15.4 with tailored MAC, ISM band 868/915 MHz	8 MB	Y	Generic, rich sensor peripherals, and wide application range

Eco, a self-contained, ultra-wearable and expandable wireless sensor platform; BSN, body sensor network; BSAN, body area sensor network; ECG, electrocardiogram; RIP, respiratory inductive plethysmograph; PPG, photoplethysmography; MAC, address resolution protocol.

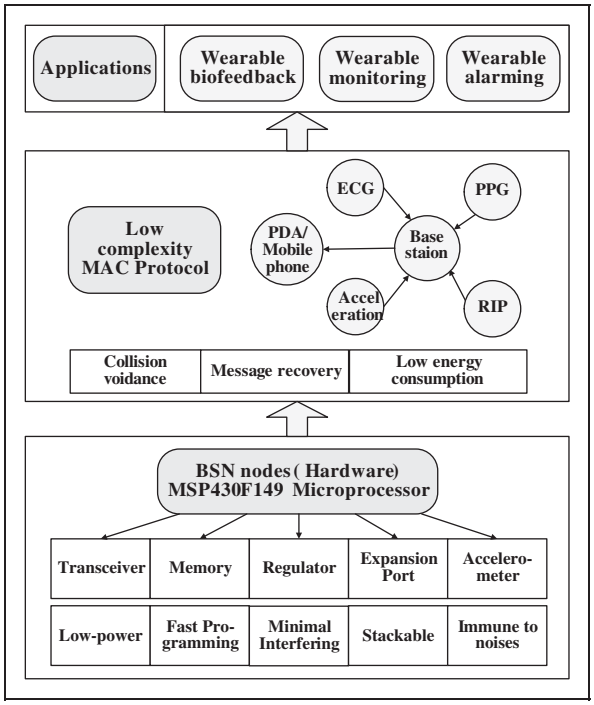

Fig. 1. The hierarchy of the generalized BSN platform we have constructed. BSN, body sensor network; ECG, electrocardiogram; PPG, photoplethysmography; RIP, respiratory inductive plethysmograph; PDA, personal digital assistant; MAC, address resolution protocol.

therapeutic exercise supporting manipulator.[19] Moore designed a handheld biofeedback device called Stress Eraser.[7] Montgomery with University of Texas suggested that slowed respiratory training could dramatically enhance the credibility of biofeedback as a treatment modality.[20] Various reports suggested that respiratory trainings have assisted patients who suffer stutters,[2] panic attacks,[3] asthmatic conditions,[4] depression,[5] and posttraumatic stress disorder.[6] As indicated in the previous section, most of these work focused on biofeedback theories and guidelines.

HARDWARE MODULES

The BSN platform included two node boards that serve as the primary BSN components; a respiratory inductive plethysmograph (RIP) sensor interface board that interfaces with an RIP belt, an ECG interface board that is capable of detecting heart rate from noncontact electrodes, a PPG sensor interface board that interfaces with conventional PPG sensor, a base station board that connects with a personal digital assistant (PDA) or mobile phone, a battery/charger board with a wireless charger that provides power supply for other boards, a compact printed circuit board (PCB) antenna whose resonant frequency was tuned to be around 900 MHz, a prototyping board for debugging, and a whip antenna. All the boards, except the base station board, were designed to be in a uniform form with 23 mm in diameter. There are well-defined expansion ports in all boards except the base station board, so these boards could be easily interconnected. *Figure 2* illustrates the complete BSN hardware platform.

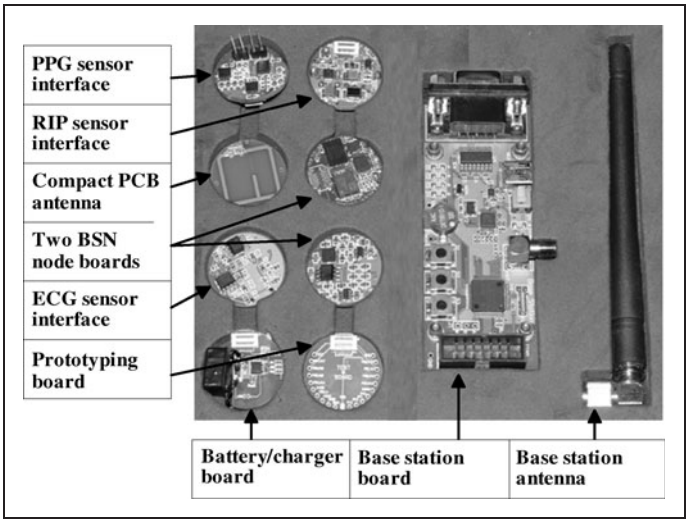

Fig. 2. Generalized BSN hardware development platform.

BSN NODE BOARD

A low-power microprocessor, a radio transceiver, a memory integrated circuit (IC), a three-dimensional (3D) accelerometer, a power regulator, a 20-pin expansion port, and affiliated discrete components were integrated on the node board. An improved address resolution protocol (MAC) was used to facilitate wireless data communication in terms of collision avoidance, message recovery, and power consumption reductions.

Microprocessor. MSP430F2418 was used because it is an ultra-low-power 16-bit reduced instruction-set computer (RISC) processor within the TI MSP430 family and it provides the best combined performance in power consumption and flexible clock subsystem.[21] In the node board, the 3D accelerometer, the flash memory chip, and the radio transceiver chip were all controlled by the microcontroller through single program initiation (SPI) ports.

Radio transceiver. IEEE 802.15.4 standard was commonly employed in most wireless sensor networks. However, relatively complicated architecture (resulting in high power consumption) proprietary limited its application for the development of BSN.[22] A Nordic nRF905 transceiver was selected because its carrier frequency is more suitable for body-proximal wireless communications and there is no proprietary protocol associated.

Memory. For BSNs it is believed that a memory bank with relatively large capacity is beneficial for data storage and buffering, because the wireless link is not reliable all the time. We used the AT25DF641, which is a 64-megabit, fast-programming, and low-power-consuming flash memory device.

Accelerometer. Detection of body motions is important for biofeedback training and physiological monitoring.[23] It could also be used to estimate energy consumptions during physical exercises. Besides, acceleration signals could be used to minimize motion artifacts when detecting vital signs parameters such as heart rate and respiration rhythm. A digital built-in three-axis accelerometer SCA3000 was embedded. This device incorporates a three-dimensional micro-electromechanical systems (3D-MEMS) element and a signal conditioning application specific integrated circuit (ASIC).[24] With its integrated design, the BSN node became more compact and immune to the noises induced by cables and connectors.

Regulator. A power regulator TPS71933-33 was used on the BSN node board for dual voltage regulations of a Li-Polymer battery in the battery board. This is beneficial because one output powers the digital portion and another supplies analog portion of the circuit board to minimize cross-interference.

Expansion port. The expansion port has 20 pins, including 8 for analog signals, 4 for generic purpose digital input/output (I/Os), 3 for SPIs, 4 for digital and analog power supplies, and 1 for battery voltage. This port enables BSN node board to connect with a variety of BSN sensor interface and battery/charger boards.

RIP, ECG, AND PPG SENSOR INTERFACE BOARDS

Respiration monitoring is vital for biofeedback trainings as well as noninvasively detecting sleep apnea and other health problems.[25] We selected a respiration sensor belt based on the advanced RIP technology. On the RIP sensor interface board, two metalized polyester film capacitors and the RIP sensor belt formed a resonance circuit whose resonance frequency varies when the shape of the RIP belt changes. A low-power DC/DC boost converter TPS61040 was used to provide 10 V voltage for the stimulation of the resonance circuit. A dual differential comparator LM393 was used to generate digital pulse outputs. The complete RIP sensor interface board is illustrated in *Figure 2*.

Heart rate monitoring using noncontact electrodes was achieved by the ECG board. The noncontact sensors, which were made of conductive fabric, were sewed on the inner side of the RIP belt. The weak voltage detected from the sensors was injected into the on-board filtering circuit, which includes the preamplifier INA118 (gain was tuned to be 11.6), one high-pass filter (cutoff frequency being 0.1 Hz), one low-pass filter (cutoff frequency being 35 Hz), and one notch filter (center frequency being 50 Hz). Subsequently, a main amplifier was used to produce variable gains. A switched capacitor voltage converter LM2664 was applied to convert the positive voltage 3.3 V to corresponding negative voltage −3.3 V.

PPG sensor interface board was designed to provide various switched driving currents for LED DLED-660/905 and to condition the weak current signals from the photodiode such as BPW34S.[26] INA118 was employed for differential transimpedance amplification. OPA2277 was used to condition the PPG signal. LM2664 was also used.

BASE-STATION BOARD

Base-station board included an MSP430F2418 microprocessor and an nRF905, which are identical to the BSN node board. Besides,

the base-station board provided RS232 and universal serial bus (USB) connections, four LEDs, and three keys for user-device interactive purposes. Once connected with a personal computer (PC) or PDA, the base-station board serves as the master node within the BSN. If the base station is connected to a PC or a PDA, the maximum distance of reliable communication was 100 m. In this study, one base station serves one patient with the sensors.

LOW-COMPLEXITY MAC PROTOCOL

A wearable biofeedback system should have a relatively small-scale structure with only two or three sensor nodes attached to the body and work within body proximal. A low-complexity MAC protocol was designed. Our design was originated from the IEEE 802.15.4 generic MAC, efforts were made toward low energy consumption and to improve the collision avoidance and message recovery performances. Further, our protocol was elaborated to facilitate the reusability of the source code and minimize the overhead of the program binary. The assembled codes only occupied 1.6-kilobyte program memory space. The communication protocol was programmed using C and so it is easy to implement other hardware platforms.

COLLISION AVOIDANCE

In a star topology, multiple sensor nodes send data to the master node simultaneously or within very short time interval; therefore, collision avoidance is of vital importance. However, the conventional carrier-sense multiple-access/collision avoidance mechanism using a four-way handshaking communication (RTS/CTS/DATA/ACK) between the sender and the receiver[27] is relatively "overweighed" when deployed in the single-master-centralized BSN, for example, the complex control overhead inevitably deteriorates the network latency. Therefore, a simplified method—the data request (DR) and ACK/DATA mechanism—was introduced.

The major change against the former arts is that our protocol was designed to be asymmetrical, that is, much of the network and protocol complexity was allocated in the master node, rather than distributed evenly among the power-constrained sensor nodes. *Figure 3a* shows a conventional collision avoidance method applied for multihop distributed computing. *Figure 3b* depicts our approach specially designed for BSN. A master node and several sensor nodes form a star network where each sensor node can only communicate with the master node. In *Figure 3b*, suppose all nodes are time synchronized, the Master sends out a DR message, and subsequently, other nodes hear the transmission of the DR. If the Node1 finds that the DR message is calling the address of its own, the Node1 sends DATA to the Master, while other nodes should sleep until the current transmission is over. Once the Master has received DATA1 beacon from Node1, it responds with an ACK1 and DR2 beacon. This time the ACK1 message denotes the acknowledgment of the Master, and DR2 shows the DR message toward Node2. In this design, the ACKX and DRX + 1 beacons were combined together as one beacon for energy savings.

As BSN nodes work within a short range, wireless link is relatively reliable and error packet rate is relatively low; in this case, our DR and ACK/DATA scheme works effectively. However, if the wireless link becomes deteriorated and the error packet rate raises, the DATA packets may lose. To maintain the data integrity, we adopted a message recovery scheme.

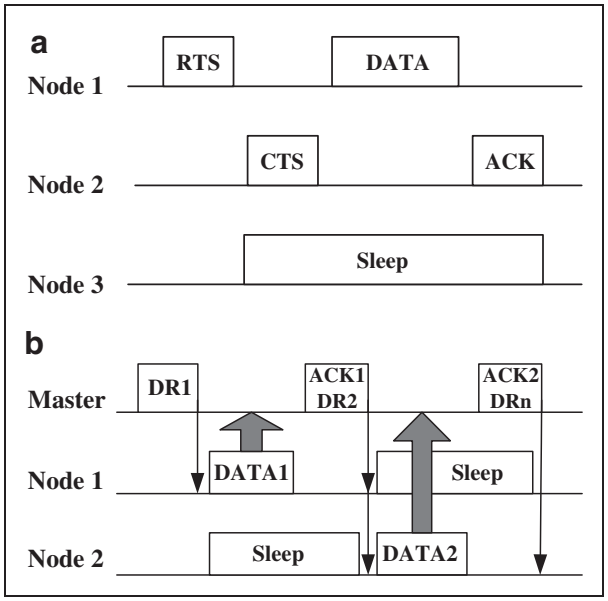

Fig. 3. Illustrations of collision avoidance of the BSN. **(a)** Conventional CSMS/CA scheme. **(b)** DR and ACK/DATA scheme. CSMS/CA, carrier sense multiple access with collision avoidance; DR, data request; ACK, acknowledgment character; CTS, clear to send; DATA, data; PCB, printed circuit board; RTS, request to send.

MESSAGE RECOVERY

Within a BSN, message loss could happen because of various situations, such as ACK loss (includes DATA loss) and DR loss. DR loss could be recovered by DR beacon retransmission. When there is an ACK loss, the certain sensor node reserves the current DATA packet in its memory, and then the new sampling DATA are shifted behind the former DATA. When the next DR beacon comes, this sensor node sends out a request for 1-plus time slot along with the DATA message for one more DR schedule from the Master. After that the Master rearranges the time schedule so that the lost message is retransmitted in the next DATA transmission pipeline. Finally, retransmissions were only allowed up to a certain limit at which the current packet should be ignored, this way the issue that leads to undesirable energy wastage was avoided.

SYSTEM INTEGRATION

A wearable biofeedback device was assembled using the aforementioned BSN modules and associated sensors, which is illustrated in details in *Figure 4*. The device could be used as a waist band or a chest band. Inside the buckle of the wearable device there was a BSN node board, sensor interface board(s), and the battery board with a Li-Polymer rechargeable battery. In the current design, the heart rate monitoring belt and the respiration monitoring belt were made separately, so that it is possible to wear one biofeedback device on the

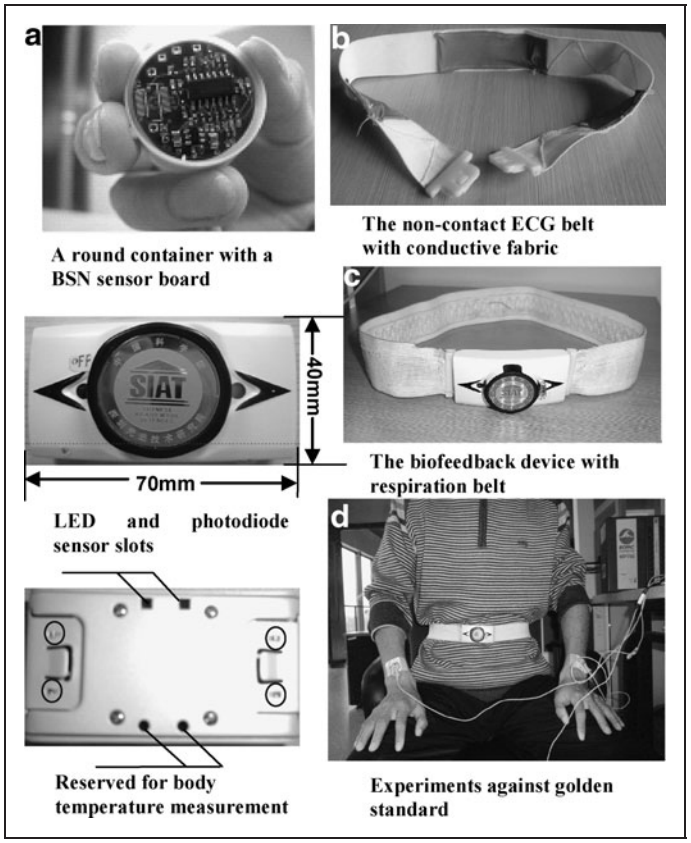

Fig. 4. Wearable devices and the verification setup. **(a)** Buckle with electronics such as BSN nodes, sensor electronics, etc.; **(b)** ECG belt with sensors; **(c)** RIP belt for respiration monitoring or biofeedback; **(d)** wearable biofeedback device and the BIOPAC verification system. The four red circles in the bottom left plot show the metal contact points that provide electrical connections between buckle and sensor belt.

thoracic level and another on the abdominal level. During experiments the wearable device(s) and the base-station formed a BSN.

System Validation

CHARACTERISTICS OF THE BSN PLATFORM

Extensive bench tests were carried to characterize the BSN platform with low-complexity MAC protocol fully implemented. During experiments, all the BSN modules were deployed around body proximal within the short communication range of < 3 m. The average power consumption of the node board at the sleep mode and the standby mode was 860 uW and 1.3 mW, respectively. The supply voltage was 3.3 V. The node worked at 915 MHz, 0 dBm, and 10 kilobits per second. The power consumptions in different transmission intervals were illustrated in *Figure 5*. Power consumptions of transmitting 32 payloads were compared using either the simplified method (our scheme) or the conventional RTS/CTS/DATA/ACK protocol. It clearly indicated that our scheme outperformed conventional protocol in terms of energy efficiency. Power savings were more

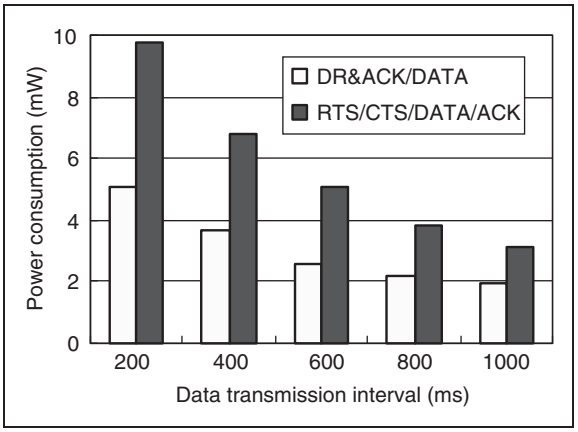

Fig. 5. Power consumptions at different data transmission intervals.

significant when shorter data transmission intervals were set. The wireless link proved to be highly reliable within body proximal.

IN-SITU PHYSIOLOGICAL MONITORING

Dynamic respiration rhythm monitoring. To evaluate respiration monitoring, a commercial product (MP150 from BIOPAC, which uses a piezoelectric sensor belt and provides a wired solution) was used for performance comparisons. In this study, the wavelet packet was used to filter high-frequency (HF) noise and baseline drift. The sampling rate for RIP signals was set at 10 samples per second. *Figure 6* depicts the respiration data acquired by the two methods. A relative mean error was calculated to be $\sim 5\%$ for this particular data episode.

In-situ dynamic respiration experiments were conducted with 10 subjects in an air-conditioned room. Subjects were at supine positions while wearing the belt around either the abdomen or the thorax.

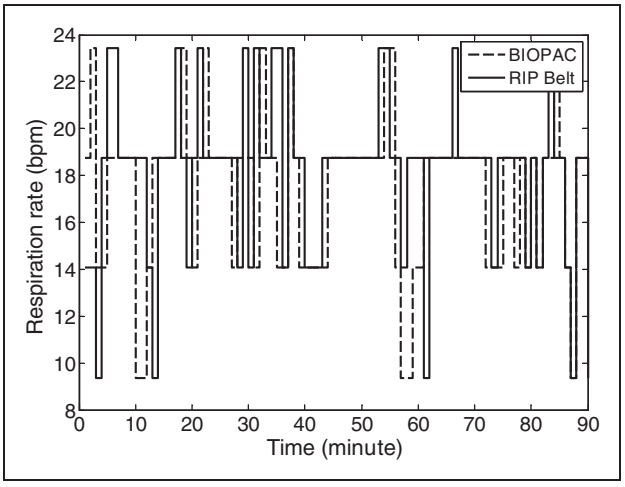

Fig. 6. The respiration data acquired from the two methods. An RSP100C module with the MP150 used piezoelectric sensor belt and provided a wired solution; the biofeedback device used digital RIP belt and wireless solution. Data were calculated every minute.

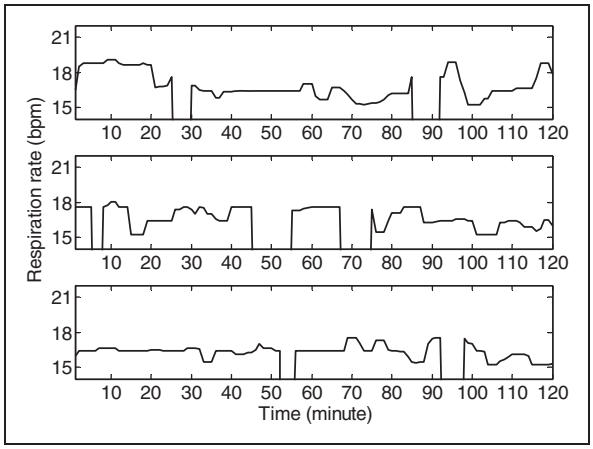

Fig. 7. The dynamic respiration rhythm of one subject over 6 h. The gap in the graph indicates the data were unable to reach the base station.

Figure 7 illustrated the 6-h dynamic respiration rate monitoring results for one subject, which indicated that ~83% of the long-term respiration rhythms were successfully detected.

SHORT-TERM PULSE RATE AND HEART RATE MONITORING

In-situ experiments for multiple subjects were carried on to evaluate short-term PPG measurement and ECG measurement. ECG100C module (using gelled electrodes) from BIOPAC was used for performance comparisons.

For PPG measurement, the subjects held the buckle of the device in one of the hands and put the thumb to cover the LED and photodiode sensor slots (*Fig. 4*). PPG signals were successfully recorded for all the subjects.

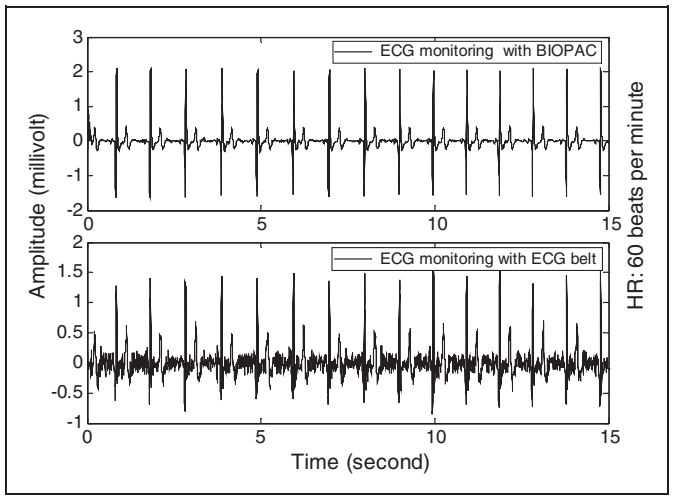

Fig. 8. Episodic ECG waveforms acquired from the two methods. ECG100C module was used with the MP150. The subject was seated under normal respiration rhythms.

For ECG measurement, the subjects worn the device with noncontact electrodes sewed on the sensor belt (*Fig. 4*). The sampling rate for ECG signals was set at 200 samples per second. A 50 Hz notch filter, a 0.5 Hz high-pass filter frequency, and a 33 Hz low-pass filter frequency were designed to filter various interferences, including of motion artifacts, power frequency, baseline drift, and electrode contact. Then, second-order (0.5–20 Hz) band pass filter, smoothing filter, and initial threshold method were used to detect exactly R-wave.

Figure 8 illustrated the episodic ECG waveforms, which indicated that our device was capable of monitoring ECG signals with noncontact electrodes. A relative error was calculated to be ~5.0% for the particular data episodes. Ten subjects participated in the 2-min experiments and the mean heart rate error was approximately 5.0%. Cardiac rhythms including heart rate and heart rate variability (HRV) were retrieved using the R-R intervals of the measured ECG signals. For long-term monitoring, ECG signals were inevitably deteriorated because of subject's motion artifacts and intermittent electrode movements.

For power consumption measurements, with a 400 mAh Li-Polymer battery (mounted within the buckle), the complete wearable biofeedback device (including the RIP and ECG interface boards, the node board, and the battery board) could operate up to 8 h, which is sufficient for continuous biofeedback training. It took 2 h for charging the battery wirelessly with the wireless charger board.

BIOFEEDBACK TRAINING

Twelve healthy students with a mean age of 24.1 years (ages between 21 and 30) have undertaken pilot studies on respiratory training. All the students submitted the SCL-90 test sheets prior to the experimental runs. The mean scores of their SCL-90s were 0.60 ± 0.23, which indicated they are all normal in terms of psychological status. All the experiments in this section were conducted in an acoustically shielded and air-conditioned room. Participants were comfortably seated during the whole experimental procedures.

Heart rate was simultaneously detected using the ECG signal, and the short-term HRV was calculated in a 120-s temporal window.[28] HRV was widely used to assess autonomic nervous system (ANS). In this experiment, two parameters, the low frequency (LF)/HF ratio and the continuous R-R interphase standard deviation (SDNN) value, were used to quantitatively represent the HRV. A spectral power analysis was carried out on R-R intervals within 120 s, based on a Fast Fourier Transformation. Absolute spectral power was calculated for two frequency bands: the LF = 0.04–0.15 Hz and the HF = 0.15–0.4 Hz. Subsequently, the LF/HF ratio was obtained. For SDNN calculations, the standard deviations of 30 continuous sinus R-R intervals were used. The sample entropy was calculated using the following equation[29]:

$$SampEn(m, \varepsilon, N) = \frac{\sum_{i=1}^{N-m+1} \log\left(\frac{N_p^m(i)}{N-m+1}\right)}{N-m+1} - \frac{\sum_{i=1}^{N-m} \log\left(\frac{N_p^{m+1}(i)}{N-m}\right)}{N-m}$$

Then, for each i,

$$N_p^m(i) = \sum_{j=1}^{N-m+1} \mathrm{cov}(i,j)$$

where m ε and N are the parameters: the embedding dimension, the SDNN and length of original data. The cov(i, j) denoted the correlation of ith and j th original data.

Considering the length of series affected the value of sample entropy. The refined sample entropy was computed by the following equation:

$$SampEn^k(m,\varepsilon,\beta) = \beta SampEn^k(m,\varepsilon,N) \cdots k = 1,2\ldots,p$$

$$\beta = 1.2 * \left(\frac{\overline{N}}{N_i}\right)^2 \cdots i = 1,2,\ldots p$$

where $\overline{N}$ denotes the mean value of the control data series.

We did the statistical tests (with SPSS v17.0) for all the experiments. Evaluations of LF/HF, SampEn, and SDNN were done with a *t*-test of independent sampler for repeated measurements. Mean and standard deviations were used to evaluate the effects in different respiratory training experiments. The inequality of variances of the differences between levels of the repeated measures factor was also tested, and the statistical significance was accepted at $p < 0.05$.

Different inhaling and exhaling ratios were evaluated using our wearable respiratory biofeedback system. They were asked to perform biofeedback trainings under three different inhaling and exhaling ratios: WB1, the ratio of inhaling and exhaling was 1.0; WB2, the ratio of inhaling and exhaling was 0.5; and WB3, the ratio of inhaling and exhaling was 2.0. The targeted respiration rate was identical for all the three tasks, that is, eight cycles per minute or 7.5 s per cycle.

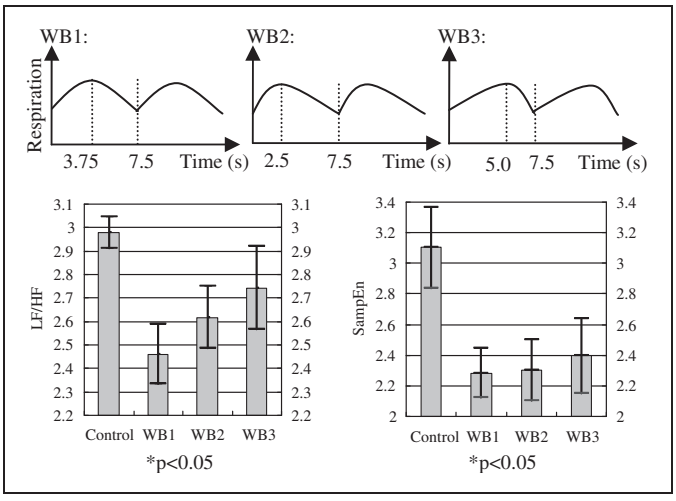

Fig. 9. Spectral (low frequency [LF]/ high frequency [HF]) and nonlinear parameters (sample entropy) were analyzed for the three wearable respiration biofeedback tasks. Mean ± one standard deviation values were plotted. The inhaling and exhaling ratio for WB1 was 1.0; the inhaling and exhaling ratio for WB2 was 0.5; and the inhaling and exhaling ratio for WB3 was 2. The different targeted respiration rhythms are illustrated at the top of this figure.

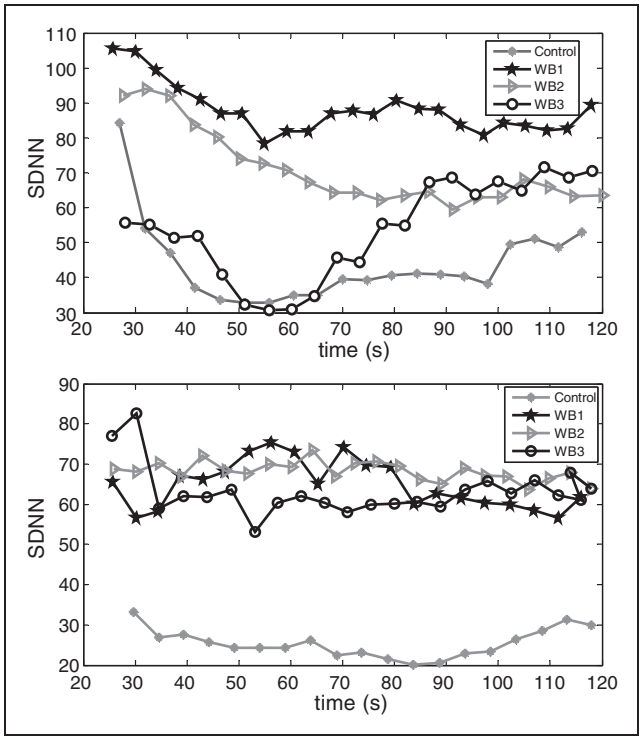

Fig. 10. Time-varying SDNN values against the time from two participants representing similar patterns. Every plot of curves was 30 continuous R-R intervals SDNN, considering temporal window.

Every task lasted for 2 min. All participants were asked to have a couple of minutes rest during the different tasks. The wearable biofeedback device was always worn at the participant's abdominal level. Results are illustrated in *Figures 9* and *10*. The LF/HF ratio, SampEn, and SDNN were calculated. The results indicated that all the tasks made contributions to the regulations of the ANS, but task 1 (inhaling and exhaling ratio being 1) had more significant effect than other two tasks (WB2 and WB3).

Different anatomical locations were also evaluated for wearable respiratory biofeedback. In this experiment, the device was worn around either the abdomen (WB1) or the thorax (WB4). Results are illustrated in *Figure 11*. For WB1 and WB4, the inhaling and exhaling ratio was set at 1.0 and the targeted respiration rhythm was eight cycles per minute or 7.5 s per cycle. The results in *Figure 12* suggested that (1) respiratory training at both abdominal level and thoracic level could affect the ANS and (2) more advanced training patterns should be explored to achieve optimal regulations of the ANS.

Discussion

DIFFERENT RESPIRATION PATTERNS

Table 2 lists the experiments with different respiration patterns. Ten participants with a mean age of 24.5 years (ages between 21 and 32) have undertaken pilot studies on respiratory training. All the students submitted the SCL-90 test sheets prior to the experimental runs. The mean scores of their SCL-90s were 0.62 ± 0.24, which

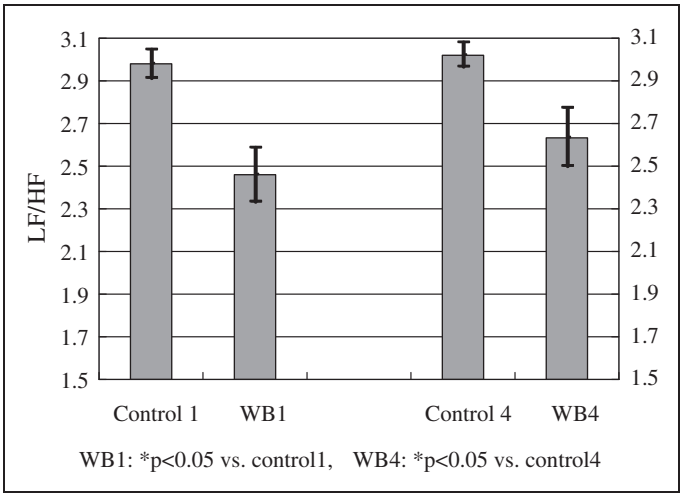

Fig. 11. LF/HF ratios at different experiments. Mean ± one standard deviation values were plotted. WB1: biofeedback at the abdominal level; WB4: biofeedback at the thoracic level.

indicated they are all normal in terms of psychological status. All the experiments in this section were conducted in an acoustically shielded and air-conditional room. Participants were comfortably seated during the whole experimental procedures.

There were no biofeedback trainings for Experiments 1 and 2 (without targeted rhythm displayed). For Experiment 3, each participant was wearing our device, while watching a screen that displayed both his or her instantaneous respiration rhythm (detected by the wearable respiratory biofeedback device worn at the participant's abdominal level and calculated in real time) and the targeted respiration rhythm, which was set at a fixed rate of eight cycles per minute or 7.5 s per cycle (the inhaling and the exhaling ratio was set at a predetermined rate of 1). The participant was expected to train himself or herself to follow the targeted respiration rhythm by watching both rhythms.

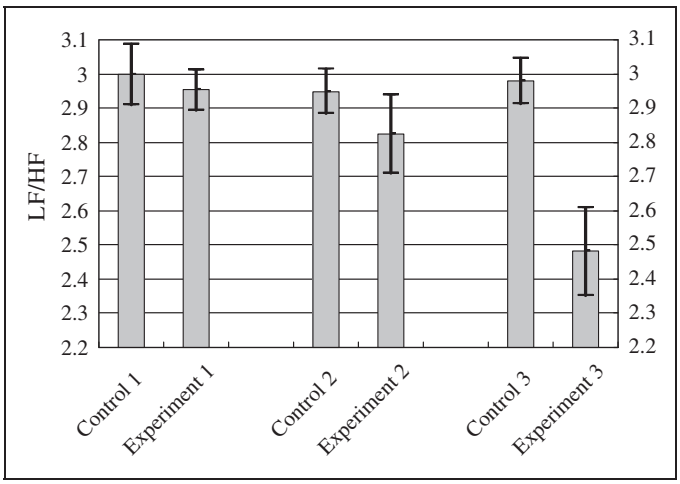

Fig. 12. The averaging LF/HF ratios for different experiments. Mean ± one standard deviation values were plotted. Experiment 1 was under natural breath; Experiment 2 was under deep breath without biofeedback; Experiment 3 was under wearable biofeedback. The detailed experiment setup is listed in *Table 2*.

Table 2. Experiments with Different Respiration Patterns

EXPERIMENT	RESPIRATION PATTERN	PROCEDURE
1	Natural breath	Sit on the chair for 2 min under natural breath (for control), 1 min under natural breath (for resting), and 2 min under the specific respiration pattern, and then, for 5 min resting among different experiments.
2	Deep breath without biofeedback	
3	Breath with wearable biofeedback	

Figure 12 demonstrated the averaging LF/HF ratios for the three experiments listed in *Table 2*. The values of $*p$ in Experiments 1 and 2 were greater than 0.05; however, the value of $*p$ in Experiment 3 was smaller than 0.05. The results indicated that only in Experiment 3, which employed our biofeedback device, the averaging LF/HF ratio was prominently reduced. Typically, the reduction of the LF/HF ratio suggested the positive effects of the regulations of sympathetic and parasympathetic nerve systems. The feasibility of ubiquitous biofeedback by using our device was verified through various experiments with different respiration patterns. Moreover, our system is superior to the conventional biofeedback devices, as it is capable of providing continuous and dynamic respiration trainings in nonclinical environments. The employment of a low-cost, generalized BSN platform makes our system easily adaptable for further biofeedback requirements.

RESPIRATORY BIOFEEDBACK

The importance of relaxed respiration, or more precisely, LF respiration (between 8 and 12 breaths per minute approximately), has been already emphasized by researches such as Benson et al.[2] or Janus et al.[30] Similarly, other researchers argued that certain dysfunctional respiratory patterns, such as shallow or hurried breathing, or more precisely, HF and low-amplitude respiratory patterns, are often associated with a wide range of psychosomatic illnesses.[31]

The study mainly compared the effectiveness of different respiratory patterns to obtain optimal respiration mode by using frequency-domain (LF/HF), time-domain (SDNN), and nonlinear analysis (sample entropy) of HRV. Those parameters, biomarkers of autonomic function and biofeedback, depended on autonomic parasympathetic and sympathetic balance. The experiments (WB1-3) demonstrated that the respiratory training with wearable biofeedback device based on our body sensor network platform effectively reduced the psychophysiological activation. Then, we deduced the conclusion that identical inhaling and exhaling ratio obtained significantly greater reductions in the cardiovascular activity than other inhaling and exhaling ratios (WB2-3). Moreover, we also found the effect of abdomen respiration

training (WB1) was similar to the effect of thorax respiration training (WB4). Thus, the pilot studies suggested that paced respiration training at abdominal level with identical inhaling and exhaling ratio (WB1) is the appropriate breath training pattern.

There are literatures reporting various experimental procedures, for example, in ref.[32] the breathing training with the inhaling/exhaling ratio being 0.66 was used in panic therapy. Parati et al. took slow breathing training with prolonged exhalation to treat patients with congestive heart failure.[33] The common concept is that the respiration training with prolonged exhaling is more beneficial than that with identical inhaling and exhaling ratio. However, it needs more contrast experiments to verify it and to obtain the optimal inhaling/exhaling ratio. In this article, our work demonstrated that WB1 (the inhaling and exhaling ratio being 1) obtained more significant reductions in the cardiovascular activities than WB2 (the inhaling and exhaling ratio being 0.5).

Conclusions

Wearable biofeedback is an emerging application field that combines modern biofeedback theories with state-of-the-art BSN technologies. The BSN platform that we have constructed is generic and has low power and low complexity, which was used to create a wearable respiratory training device. Extensive bench and *in-situ* testing results concluded that the platform and the device worked as intended. The pilot study was conducted on wearable training patterns and resultant HRV. The results in all the experiments suggested that paced respirations at abdominal level and with identical inhaling and exhaling ratio was appropriate for decreasing sympathetic arousal and increasing parasympathetic activity. We believe that the BSN platform and the wearable device could facilitate the research and development activities for ubiquitous and low-cost healthcare. In the future we will investigate more advanced infrastructure of the BSN-based biofeedback systems by using multiple physiological parameters.

Acknowledgments

These authors are sincerely thankful to Prof. Y.T. Zhang and Ms. D. Wu, for their assistance in conducting the study. This work was supported in part by Chinese Academy of Sciences "the 100 Talent People" program, the Projects of National Natural Science Foundation of China (Grant Nos. 60932001 and 61072031), the National Basic Research (973) Program of China (Sub-grant 6 of Grant No. 2010CB732606) and the Knowledge Innovation Program of the Chinese Academy of Sciences.

Disclosure Statement

No competing financial interests exist.

REFERENCES

1. Conner SJ, Sullo E, Sheeler R. How can you prevent migraines during pregnancy. *J Fam Pract* **2006;**55:429–432.
2. Benson H, Beary JG, Carol MP. The relaxation response. *Psychiatry* **1974;**37: 57–76.
3. Clark DM, Salkovskis PM, Chalkley AJ. Respiratory control as a treatment for panic attacks. *J Behav Ther Exp Psychiatry* **1985;**16:23–30.
4. Steptoe A, Phillips J, Harling J. Biofeedback and instructions in the modification of total respiratory resistance: An experimental study of asthmatic and no asthmatic volunteers. *J Psychosom Res* **1981;**25:541–551.
5. Martin S, Volkan A, Jana U, Katja P, Michael MW. A Pilot study on the effects of heart rate, variability biofeedback in patients with depression and in health subjects. *Appl Psycholphysiol Biofeedback* **2008;**33:195–201.
6. Terri LZ, Kristin WS, Richard NG. The effects of respiratory sinus arrhythmia biofeedback on heart rate variability and posttraumatic stress disorder symptoms: A pilot study. *Appl Psychophysiol Biofeedback* **2009;**34:135–143.
7. Moore SK. Calm in your palm: Biofeedback device promises to reduce stress. *IEEE Spectr* **2006;**43:60.
8. Yang GZ. *Body sensor networks*. London: Springer-Verlag, **2006**.
9. Natarajan A, Motani M, Chua KC. Investigating network architectures for body sensor networks. Conference on Mobile Systems. **2007;**19–24.
10. DeVaul R, Sung M, Pentland A. MIThril 2003: Applications and architecture. Proceedings of 7th IEEE International Symposium on Wearable Computers. **2003;**4–11.
11. Chulsung P, Chou PH. Eco: Ultra-wearable and expandable wireless sensor platform. Presented at IEEE Workshop on Wearable and Implantable Body Sensor Networks. **2006;**161–165.
12. Kuryloski P, Giani A, Bajcsy R. DexterNet: An open platform for heterogeneous body sensor networks and its applications. Presented at IEEE Workshop on Wearable and Implantable Body Sensor Networks. **2009;**92–97.
13. Seto EYW, Giani A, Bajcsy R. A wireless body sensor network for the prevention and management of asthma. Presented at IEEE Symposium on Industrial Embedded Systems. **2009;**120–123.
14. King RC, Atallah L, Yang GZ. Development of a wireless sensor glove for surgical skills assessment. *IEEE Trans Inf Technol Biomed* **2009;**13: 673–679.
15. Barth AT, Hanson MA, Lach J. TEMPO 3.1: A body area sensor network platform for continuous movement assessment. Presented at IEEE Workshop on Wearable and Implantable Body Sensor Networks. **2009;**71–76.
16. Lin Z, Sinclair M, Bittner R. A phone-centered body sensor network platform cost, energy efficiency & user interface. *Presented at IEEE Workshop on Wearable and Implantable Body Sensor Networks*. **2006;**179–182.
17. Yokoyama K, Ushida J, Takata K. Heart rate indication using musical data. *IEEE Trans Biomed Eng* **2002;**49:729–733.
18. Dozza M, Chiari L, Horak FB. Effects of linear versus sigmoid coding of visual or audio biofeedback for the control of upright stance. *IEEE Trans Neural Syst Rehabil* **2006;**14:505–512.
19. Komada S, Hashimoto Y, Hirai J. Development of a biofeedback therapeutic-exercise-supporting manipulator. *IEEE Trans Ind Electron* **2009;**56: 3914–3920.
20. Montgomery GT. Slowed respiration training. Biofeedback Self Regul **1994;**19:211–225.
21. MSP430x13x, MSP430x14x, MSP430x14x1 Mixed Signal Microcontroller. Texas Instruments. **2004**. Available at http://focus.ti.com/docs/prod/folders/print/msp430f149.html.
22. Li YZ, Wang L, Zhang YT. Experimental analysis on radio transmission and localization of a Zigbee-based wireless healthcare monitoring platform. *Proceedings of 5th International Conference on Information Technology and Application in Biomedicine*. China, **2008;**488–490.
23. Aziz O, Wang L, Yang GZ, Darzi A. A pervasive body sensor network for measuring postoperative recovery at home. *Surg Innov* **2007;**14:83–90.
24. SCA3000-D01 3-AXIS LOW POWER ACCELEROMETER WITH DIGITAL SPI INTERFACE. VTI Technology. Available at www.vti.fi/en/.

25. Wu D, Wang L, Zhang YT. A wearable respiration monitoring system based on digital respiratory inductive plethysmography. International Conference of the Engineering in Medicine and Biology Society. **2009;**4844–4847.

26. Wang L, Lo BPL, Yang GZ. Multichannel reflective PPG earpiece sensor with passive motion cancellation. *IEEE Trans Biomed Circuits Syst* **2007;**1:235–241.

27. Sun LM, Chen Y, Zhu HS. *Wireless sensor networks*. Beijing: Tsinghua University Press, **2005**.

28. Camm J, Malik M, et al. Heart rate variability: Standards of measurement, physiological interpretation and clinical use. *Circulation* **1996;**93:1043–1065.

29. Miguel AGG, Mireya FC, Juan RC. Errors in the estimation of approximate entropy and other recurrence-plot-derived indices due to the finite resolution of RR time series. *IEEE Transl Biomed Eng* **2009;**56:345–351.

30. Janus I, Defares P, Grossman P. Hypervigilant reactions to threat. In: Selye H, ed. *Selye guide to stress research*, vol. 3. New York: Scientific and Academic Editions, **1987**.

31. Grossman P. Respiration, stress, and cardiovascular function. *Psychophysiology* **1983;**3:284–300.

32. Parati G, Malfatto G, et al. Device-guided paced breathing in the home setting: Effects on exercise capacity, pulmonary and ventricular function in patients with chronic heart failure: A pilot study. *Circ Heart Fail* **2008;**1:178–183.

33. Meuret AE, Wilhelm FH, Roth WT. Respiratory biofeedback-assisted therapy in panic disorder. *Behav Modif* **2001;**25:584–605.

Address correspondence to:
Lei Wang, Ph.D.
Institute of Biomedical and Health Engineering
Shenzhen Institutes of Advanced Technology
Chinese Academy of Sciences
Shenzhen 518055
China

E-mail: wang.lei@siat.ac.cn

Received: October 20, 2010
Revised: December 30, 2010
Accepted: January 3, 2011